J. Coat. Technol. Res., **8** (6) 685–695, 2011
DOI 10.1007/s11998-011-9341-2

3-Methyl-4-amino-5-mercapto-1,2,4-triazole as corrosion inhibitor for 6061 Al alloy in 0.5 M sodium hydroxide solution

P. D. Reena Kumari, Jagannath Nayak, A. Nityananda Shetty

Abstract 3-Methyl-4-amino-5-mercapto-1,2,4-triazole (MAMT) was synthesized, and its inhibition action on the corrosion of 6061 Al alloy in 0.5 M sodium hydroxide was investigated by means of potentiodynamic polarization and electrochemical impedance spectroscopy techniques. The effect of inhibitor concentration, temperature, and concentration of the corrosion medium on the inhibitor action was investigated. The surface morphology of the metal surface was investigated by scanning electron microscopy (SEM). The inhibition efficiency increased with the increase in the concentration of the inhibitor, but decreased with the increase in temperature. Both thermodynamic and kinetic parameters were calculated and discussed. The adsorption of MAMT on the base alloy was found to be through physisorption, obeying Langmuir's adsorption isotherm. The results obtained from both the techniques were in good agreement with each other.

Keywords Alloys, Corrosion inhibition, Electrochemical techniques, Adsorption isotherm

P. D. R. Kumari
Department of Chemistry, Srinivas School of Engineering, Mukka, Mangalore 575 025, Karnataka, India

J. Nayak
Department of Metallurgical & Materials Engineering, National Institute of Technology Karnataka, Surathkal, Srinivasnagar 575 025, Karnataka, India

A. N. Shetty (✉)
Department of Chemistry, National Institute of Technology Karnataka, Surathkal, Srinivasnagar 575 025, Karnataka, India
e-mail: nityashreya@gmail.com

Introduction

Aluminum alloy 6061 is one of the most extensively used 6000 series aluminum alloys. It is widely used for the construction of aircraft structures, yacht construction, bicycle frames, machinery and process-equipment applications. Al 6061 alloy contains magnesium and silicon as its major alloying elements. It is a versatile heat-treatable alloy with medium-to-high strength capabilities, satisfying the requirements of a number of specifications in extruded shape. Owing to its wide applicability in industrial and everyday life, the electrochemical properties of aluminum and its alloys are the topics of many research studies.[1–7] However, corrosion is indeed one of the major problems affecting the performance and safety of the metal. Several methods have been devised for preventing or reducing corrosion, which include metal coating, inorganic coating, painting, as well as use of chemical inhibitors. The uses of some organic and inorganic compounds as effective inhibitors to protect metallic materials in the environment containing aggressive ions have been reported. It is reported that many organic compounds containing hetero atoms like N, O, S, and multiple bonds in their molecule have been proven to be effective inhibitors for the corrosion of aluminum alloys in acid and alkaline media.[8–15] In general, it has been assumed that the action of inhibitors in aggressive media is by the adsorption of the inhibitors onto the metal surface. The processes of adsorption of inhibitor are influenced by the nature and surface charge of the metal, the chemical structure of organic inhibitors, the type of aggressive electrolyte and the type of interaction between organic molecules and the metallic surface.[16]

The search in the literature reveals little study being reported on corrosion inhibition studies on 6061 aluminum alloy in sodium hydroxide medium. Aluminum and its alloys are highly susceptible to corrosion

in the alkaline media. Therefore, it is important to study the corrosion control of aluminum alloys in alkaline media using suitable inhibitors. 1,2,4-Triazoles and their derivatives are incorporated into a wide variety of therapeutically important compounds possessing a broad spectrum of biological activities and many other applications including corrosion inhibition of metals.[17,18] These compounds can be adsorbed on a metal surface not only through lone pairs of electrons on nitrogen or sulfur atoms but also through pi electrons present in these molecules.[19] The purpose of this article is to determine the influence of 3-methyl-4-amino-5-mercapto-1,2,4-triazole (MAMT) on the corrosion of 6061 Al alloy in sodium hydroxide solution, using potentiodynamic polarization and electrochemical impedance techniques. The effects of temperature and inhibitor concentration were studied, and several isotherms were tested for their relevance to describe the adsorption behavior of the compound studied.

Experimental

Materials and chemicals

The material employed was 6061 Al alloy in extruded rod form (extrusion ratio 30:1). The chemical composition of the 6061 aluminum alloy is given in Table 1. The sample was metallographically mounted up to 10-mm height using cold setting epoxy resin, so that the exposed surface area of the metal to the media was 0.785 cm^2. These coupons were polished as per standard metallographic practice-belt grinding followed by polishing on emery papers of 400, 600, 800, 1000, 1200, and 1500 grades, finally on a polishing wheel using levigated alumina to obtain a mirror finish degreased with acetone, washed with double distilled water, and dried before immersing in the corrosion medium. For the electrochemical measurement, the arrangement comprised a conventional three electrode Pyrex glass cell with a platinum counter electrode and a saturated calomel electrode (SCE) as reference. The test solution used for the investigation was standard solution of 0.5 M sodium hydroxide prepared by using sodium hydroxide pellets of AR grade and double distilled water.

Synthesis of MAMT

The MAMT was synthesized and recrystallized as per the reported procedure in a one-step reaction of thiocarbohydrazide and glacial acetic acid.[20] A mixture of thiocarbohydrazide (10 g) and acetic acid (60 mL) was taken in a round-bottomed flask. The reaction mixture was refluxed for about 4 h. The precipitated product was purified by recrystallization from hot water and was identified by melting point (203–204°C), elemental analysis, and infrared spectra. The molecular weight of the compound is 130. The structure of the molecule is shown in Fig. 1. For the inhibition studies, MAMT was dissolved in 0.5 M sodium hydroxide in appropriate quantities.

Table 1: The chemical composition of the 6061 Al alloy

Element	Cu	Si	Mg	Cr	Al
Composition (wt%)	0.25	0.6	1.0	0.25	Balance

Potentiodynamic polarization method

Electrochemical measurements were carried out using electrochemical work station, GillAC, and ACM Instruments Version 5 software. Tafel plot measurements were carried out using conventional three electrode Pyrex glass cell with platinum counter electrode, and saturated calomel electrode (SCE) as reference electrode. All the values of potential are, therefore, referred to the SCE. Finely polished composite specimens were exposed to the corrosion medium of sodium hydroxide in the absence and presence of inhibitor at different temperatures (30–50°C) and allowed to establish a steady-state open circuit potential (OCP). The potentiodynamic current–potential curves were recorded by polarizing the specimen to −250 mV cathodically and +250 mV anodically with respect to OCP at a scan rate of 1 mV s^{-1}.

Electrochemical impedance spectroscopy studies (EIS)

The corrosion behaviors of specimens of the base alloy were also obtained from EIS technique. In the EIS technique, a small amplitude ac signal of 10 mV with the frequency spectrum ranging from 100 kHz to 0.01 Hz was impressed at the OCP and impedance data were analyzed using Nyquist plots. The polarization resistance was extracted from the diameter of the semicircle in Nyquist plot.

In all the above measurements, at least three similar results were considered and their average values are reported.

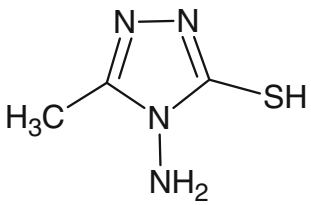

Fig. 1: The molecular structure of 3-methyl-4-amino-5-mercapto-1,2,4-triazole

Scanning electron microscopy (SEM) analysis

The scanning electron microscope images of the samples were recorded using JEOL JSM-6380 LA analytic scanning electron microscope.

Results and discussion

Potentiodynamic polarization method

The polarization studies of the alloy specimens were investigated in 0.5 M NaOH solution containing various concentrations of MAMT at different temperatures using Tafel polarization technique. Figure 2 shows the Tafel polarization curves for the corrosion of the alloy in 0.5 M NaOH solution at 30°C devoid of and containing different concentrations of MAMT. Similar plots were obtained at the other temperatures studied. The percentage inhibition efficiency (%IE) was calculated from the expression (1).

$$\%\mathrm{IE} = \frac{i_{\mathrm{corr}_{(\mathrm{uninh})}} - i_{\mathrm{corr}_{(\mathrm{inh})}}}{i_{\mathrm{corr}_{(\mathrm{uninh})}}} \times 100 \qquad (1)$$

where $i_{\mathrm{corr}_{(\mathrm{uninh})}}$ and $i_{\mathrm{corr}_{(\mathrm{inh})}}$ are the corrosion current densities in the absence and presence of the inhibitor, respectively. The corrosion rate is calculated using the equation (2):

$$\text{Corrosion rate } (\mathrm{mm\,year^{-1}}) = \frac{3270 \times M \times i_{\mathrm{corr}}}{\rho \times Z} \qquad (2)$$

where 3270 is a constant that defines the unit of corrosion rate, i_{corr} is the corrosion current density in A $\mathrm{cm^{-2}}$, ρ is the density of the corroding material (g $\mathrm{cm^{-3}}$), M is the atomic mass of the metal, and Z is the number of electrons transferred per atom.[21]

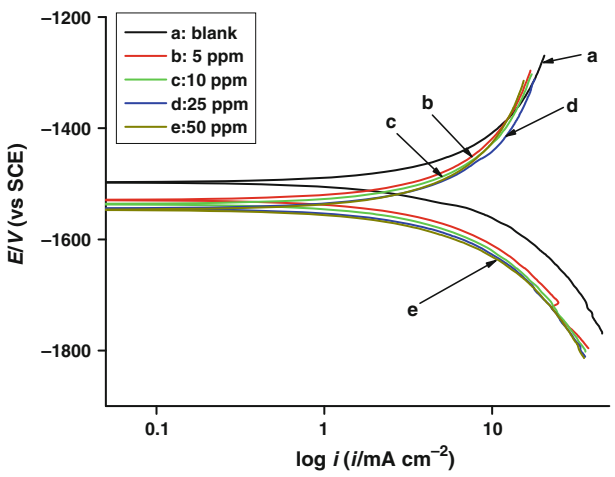

Fig. 2: Potentiodynamic polarization curves for the corrosion of 6061 Al alloy in 0.5 M NaOH at 30°C in the presence of different concentrations of MAMT

The electrochemical parameters including corrosion potential (E_{corr}), corrosion current density (i_{corr}), corrosion rate (CR), anodic and cathodic slopes (b_{a} and b_{c}), and inhibition efficiency (%IE) calculated from Tafel plots are summarized in Table 2. As can be seen from the data, addition of MAMT decreases the corrosion of the base alloy sample. Inhibition efficiency increases with the increase in MAMT concentration. The changes in both the anodic and cathodic Tafel slopes observed on the addition of MAMT indicate that both anodic and cathodic reactions are affected by the addition of the inhibitor. It is also seen that the addition of MAMT shifts the E_{corr} values toward more negative potential, indicating predominant cathodic inhibition action by MAMT. According to Ferreira et al.[22,23] and Li et al.[22,23] if the displacement in corrosion potential is more than ±85 mV with respect to corrosion potential of the blank, then the inhibitor can be considered as a cathodic or an anodic type. However, the maximum displacement in this study is −67 mV, which indicates that MAMT is a mixed type inhibitor with predominant control of the cathodic reaction.[24,25] The parallel cathodic Tafel curves in Fig. 2 suggest that the cathodic reaction is activation-controlled and reduction mechanism is not affected by the presence of the inhibitor.[26] The values of b_{c} change with the increasing inhibitor concentration, which indicates the influence of the compound on the kinetics of cathodic reaction. The shift in the anodic Tafel slope b_{a} may be due to the inhibitor molecules adsorbed on the metal surface.[27]

Effect of temperature

The effect of temperature on the inhibited electrolyte–metal reaction is highly complex because many changes occur on the metal surface, such as desorption of the inhibitor molecules, which in some cases may undergo decomposition and/or rearrangement.[28] However, it facilitates the calculation of many thermodynamic parameters for the inhibition and for the adsorption processes which contribute to determining the type of adsorption of the studied inhibitors. In the present study, with the increase in solution temperature, corrosion current density (i_{corr}) and hence the corrosion rate of the specimen increases in both the blank and the inhibited solutions. The inhibition efficiency decreases with the increase in temperature which indicates desorption of inhibitor molecules.[29] However, this decrease is small at a higher concentration of inhibitor. The apparent activation energy (E_{a}) for the corrosion process in the presence and the absence of inhibitor can be calculated using Arrhenius Law in equation (3).

$$\ln(\mathrm{CR}) = -E_{\mathrm{a}}/RT + A \qquad (3)$$

where A is the Arrhenius preexponential factor, E_{a} is the activation energy of the corrosion process, R is the universal gas constant, and T is the absolute temperature. The plot of ln(CR) vs reciprocal of

Table 2: Tafel results for the corrosion of 6061 Al alloy in 0.5 M sodium hydroxide in the presence of MAMT at different temperatures

Temperature (°C)	Inhibitor concentration (ppm)	E_{corr} (mV SCE^{-1})	b_a (mV dec^{-1})	$-b_c$ (mV dec^{-1})	i_{corr} (mA cm^{-2})	CR (mm year^{-1})	IE (%)
30	0	−1501	313	289	5.57	61.15	–
	5	−1529	195	153	3.04	33.32	45.5
	10	−1536	178	146	2.78	30.53	50.1
	25	−1544	156	133	2.51	27.49	55.0
	50	−1547	142	117	2.11	23.16	62.1
35	0	−1492	323	293	6.10	66.89	–
	5	−1526	195	184	3.58	39.29	41.3
	10	−1537	161	157	3.26	35.73	46.6
	25	−1542	143	142	2.89	31.68	52.6
	50	−1549	156	126	2.67	29.28	55.6
40	0	−1496	308	281	6.63	72.71	–
	5	−1519	150	102	3.96	43.45	40.2
	10	−1540	163	151	3.63	39.80	45.3
	25	−1545	156	143	3.45	37.90	47.9
	50	−1548	151	135	3.00	32.93	54.7
45	0	−1481	262	265	7.04	77.20	–
	5	−1530	212	158	4.41	48.39	37.3
	10	−1538	159	154	4.08	44.80	42.0
	25	−1547	143	127	3.86	42.35	45.1
	50	−1548	123	143	3.48	38.19	50.5
50	0	−1496	320	359	8.98	98.55	–
	5	−1533	186	202	5.86	64.27	34.8
	10	−1537	193	168	5.34	58.62	40.5
	25	−1541	120	119	5.08	55.70	43.5
	50	−1551	164	135	4.77	52.37	46.9

absolute temperature ($1/T$) gives a straight line whose slope, $-E_a/R$, gives activation energy for the corrosion process. The Arrhenius plots for the corrosion of the alloy are shown in Fig. 3. The entropy and enthalpy of activation values for the dissolution of the alloy (ΔH_a and ΔS_a) were calculated from transition state theory (equation (4)).

$$\mathrm{CR} = \frac{RT}{Nh}\exp\left(\frac{\Delta S_a}{R}\right)\exp\left(\frac{-\Delta H_a}{R}\right) \quad (4)$$

where h is Planck's constant, and N is Avogadro's number. A plot of $\ln(\mathrm{CR}/T)$ vs $1/T$ gives a straight line with slope equal to $-\Delta H_a/R$ and intercept equal to $\ln(R/Nh) + \Delta S_a/R$. The plots of $\ln(\mathrm{CR}/T)$ vs $1/T$ for the corrosion of the alloy in 0.5 M NaOH in the presence of different concentrations of inhibitor are shown in Fig. 4. The calculated values of the apparent activation energy E_a, activation enthalpy ΔH_a, and activation entropy ΔS_a are given in Table 3.

The effect of chemically stable surface active inhibitors is to increase the energy of activation and to decrease the surface area available for corrosion.[30] The results in Table 3 indicate that the value of activation energy (E_a) in 0.5 M NaOH solution containing inhibitor is greater than that without the inhibitor. The increase in the activation energies with the

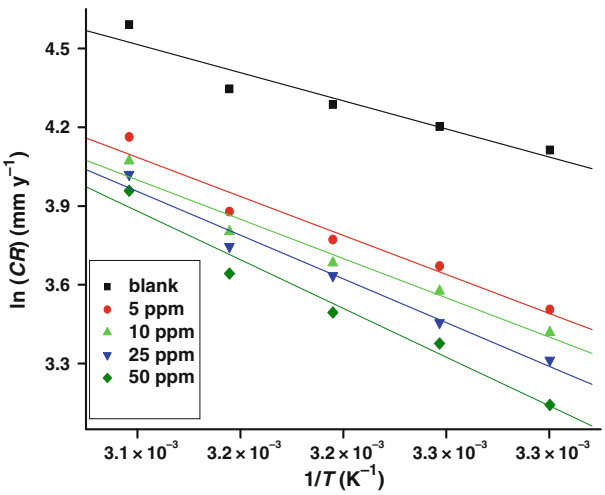

Fig. 3: Arrhenius plots for the corrosion of 6061 Al alloy in 0.5 M NaOH in the presence of different concentrations of MAMT

increase in the concentration of the inhibitor is attributed to the adsorption of inhibitor molecules on the metal surface. There is an appreciable increase in the adsorption process of the inhibitor on the metal surface with the increase in the concentration of the

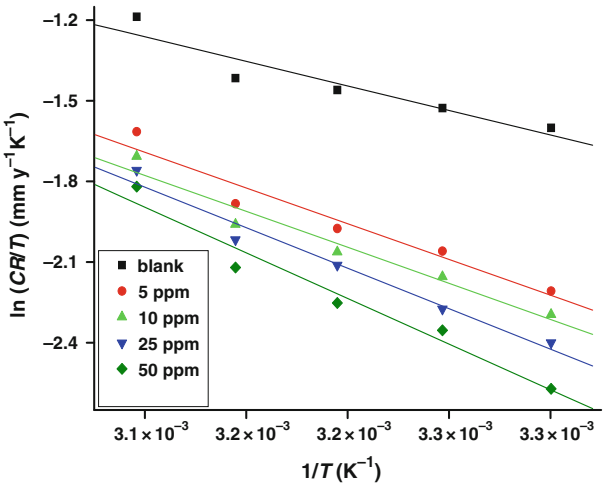

Fig. 4: ln(CR/*T*) vs 1/*T* plots for the corrosion of 6061 Al alloy in 0.5 M NaOH in the presence of different concentrations of MAMT

Table 3: Activation parameters for the corrosion of 6061 Al alloy in 0.5 M sodium hydroxide solution in the presence of MAMT

Inhibitor concentration (ppm)	E_a (kJ mol^{-1})	ΔH_a (kJ mol^{-1})	$-\Delta S_a$ (J mol^{-1} K^{-1})
0	17.79	15.19	160.98
5	24.70	22.10	143.12
10	24.85	22.25	143.37
25	27.65	25.05	135.06
50	30.83	28.23	125.83

inhibitor,[31] thereby increasing the activation energies. The adsorption of the inhibitor molecules on the surface of the metal blocks the charge transfer during corrosion reaction, thereby increasing the activation energy.[32] In other words, the adsorption of the inhibitor on the electrode surface leads to the formation of a physical barrier that reduces the metal reactivity in the electrochemical reactions of corrosion.[33] The decrease in the inhibition efficiency of MAMT with increase in temperature can be attributed to an appreciable decrease in the adsorption of the inhibitor on the metal surface with increase in temperature and corresponding increase in corrosion rate because a greater area of the metal is exposed to the corrosion medium. The observations also suggest physisorption of the inhibitor molecules on the surface of the alloy.

The entropy of activation values in the absence and presence of inhibitor are negative. This implies that the activated complex in the rate-determining step represents an association rather than a dissociation step, resulting in a decrease in randomness on going from reactants to activated complex.[15] The entropy of activation values are less negative for inhibited solutions than for the uninhibited solutions. This suggests that an increase in randomness occurred while moving from reactants to the activated complex in the presence of the inhibitor. This might be the result of the adsorption of organic inhibitor molecules from the alkaline medium, which could be regarded as a quasi-substitution process between the organic compound in the aqueous phase and water molecules at the electrode surface.[34] In this situation, the adsorption of organic inhibitor is accompanied by desorption of water molecules from the surface. Thus, the increase in entropy of activation may be attributed to the increase in solvent entropy.[35]

Adsorption behavior

Organic corrosion inhibitors are known to decrease metal dissolution via adsorption on the metal/corrodent interface to form a protective film which separates the metal surface from the corrosive medium. The adsorption route is usually regarded as a substitution process between the organic inhibitor in the aqueous solution [In $h_{(sol)}$] and water molecules adsorbed at the metal surface [$H_2O_{(ads)}$] as given below[36]

$$\text{In}\, h_{(sol)} + \chi H_2O_{(ads)} \leftrightarrow \text{In}\, h_{(ads)} + \chi H_2O_{(sol)} \quad (5)$$

where χ represents the number of water molecules replaced by one molecule of an adsorbed inhibitor. The adsorption bond strength is dependent on the composition of the metal, corrodent, inhibitor structure, concentration, and orientation as well as temperature. Basic information on the interaction between the inhibitor and metal surface can be provided by the adsorption isotherm. The degrees of surface coverage (θ) in the presence of different concentrations of inhibitor were evaluated from potentiodynamic polarization measurements. The data were applied to various isotherms including Langmuir, Temkin, Frumkin, and Flory–Huggins isotherms. By far, the best fit was obtained with the Langmuir adsorption isotherm. The Langmuir adsorption isotherm could be represented by the equation:

$$\frac{C}{\theta} = C + \frac{1}{K} \quad (6)$$

where K is the adsorption/desorption equilibrium constant, C is the corrosion inhibitor concentration in the solution, and θ is the surface coverage, which is calculated using equation (7).

$$\theta = \frac{\%\text{IE}}{100} \quad (7)$$

where %IE is the percentage inhibition efficiency as calculated using equation (1). Taking the logarithm of both the sides of equation (6), equation (8) is obtained.

$$\log\left(\frac{C}{\theta}\right) = \log C - \log K \quad (8)$$

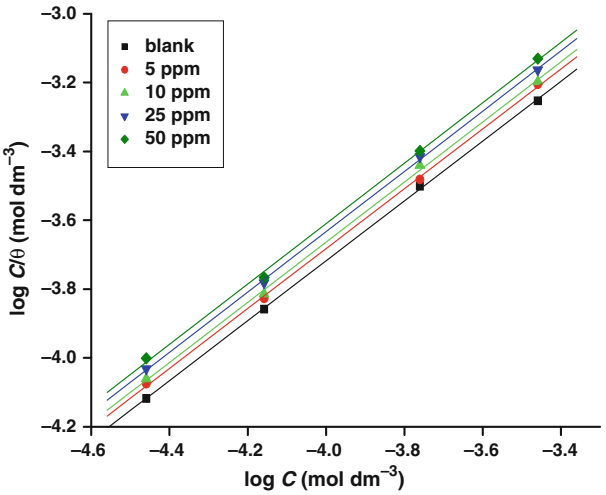

Fig. 5: Langmuir adsorption isotherms for the adsorption of MAMT on the alloy surface

The plot of $\log(C/\theta)$ vs $\log C$ gives a straight line with intercept equal to $-\log K$. The Langmuir adsorption isotherms are shown in Fig. 5. The slopes show deviation from the value of unity as would be expected for the ideal Langmuir adsorption isotherm equation. This deviation from unity may be due to the interaction among the adsorbed species on the metal surface and also due to the nonhomogeneous surface conditions of the alloy. It has been postulated in the derivation of the Langmuir isotherm equation that adsorbed molecules do not interact with one another, but this is not true in the case of organic molecules having polar atoms or groups which are adsorbed on the cathodic and anodic sites of the metal surface. Such adsorbed species may interact by mutual repulsion or attraction. It is also possible that the inhibitor molecules studied can be differentially adsorbed on the anodic and cathodic sites resulting in deviation from unit gradient. Similar results have been reported by Sethi et al.[37] The thermodynamic parameter, standard free energy of adsorption, (ΔG°_{ads}) is calculated from the thermodynamic equation

$$K = \frac{1}{55.5}\exp\left(\frac{-\Delta G^{\circ}_{ads}}{RT}\right) \quad (9)$$

where K is the equilibrium constant for the adsorption/desorption process, 55.5 mol dm^{-3} is the molar concentration of water in the solution, T is temperature, and R is the gas constant.[38,39]

Standard enthalpy of adsorption (ΔH°_{ads}) and standard entropies of adsorption (ΔS°_{ads}) were obtained from the plot of (ΔG°_{ads}) vs T according to the thermodynamic basic equation

$$\Delta G^{\circ}_{ads} = \Delta H^{\circ}_{ads} - T\Delta S^{\circ}_{ads} \quad (10)$$

The values of standard free energy adsorption (ΔG°_{ads}), standard enthalpy of adsorption (ΔH°_{ads}), standard entropy of adsorption (ΔS°_{ads}), and equilibrium constant (K) are listed in Table 4. The enthalpy of adsorption could be approximately regarded as the standard enthalpy of adsorption (ΔH°_{ads}) under experimental conditions.[40] The negative sign of ΔH°_{ads} in NaOH solution indicates that the adsorption of inhibitor molecule is an exothermic process. In general, an exothermic adsorption process signifies either physisorption or chemisorption while endothermic process is attributable unequivocally to chemisorptions.[41] Typically, the enthalpy of physisorption process is less negative than -41.86 kJ mol^{-1}, while the enthalpy of chemisorptions process approaches -100 kJ mol^{-1}.[42] In the present study, the value of enthalpy is -13.30 kJ mol^{-1} which suggests that the adsorption of MAMT on 6061 Al alloy involves a physisorption phenomenon.

Table 4: Thermodynamic parameters for the adsorption of MAMT on 6061 Al alloy surface in 0.5 M sodium hydroxide solution

Temperature (°C)	log K	$-\Delta G^{\circ}_{ads}$ (kJ mol^{-1})	$-\Delta H^{\circ}_{ads}$ (kJ mol^{-1})	$-\Delta S^{\circ}_{ads}$ (J mol^{-1} K^{-1})
30	0.2400	11.51		
35	0.2030	11.48		
40	0.1701	11.47	13.30	58.70
45	0.1306	11.42		
50	0.0989	11.40		

The negative values of ΔG°_{ads} indicate the spontaneity of the adsorption process and stability of the adsorbed layer on the metal surface. In general, the values of ΔG°_{ads} around -20 kJ mol^{-1} are consistent with physisorption, while those around -40 kJ mol^{-1} or higher correspond to chemisorptions.[43,44] The calculated values of ΔG°_{ads} obtained in this study are close to -11.50 kJ mol^{-1} indicating physical adsorption of MAMT on the aluminum alloy surface. Also, the decreases in the inhibition efficiency (%IE) with the increase in temperature, as observed in this study, is indicative of physical adsorption.

Electrochemical impedance spectroscopy (EIS) studies

In order to get more information about the corrosion inhibition of 6061 Al alloy specimens in 0.5 M NaOH containing different concentrations of MAMT, EIS measurements were carried out at different temperatures. The Nyquist plots obtained for the corrosion of 6061 Al alloy in 0.5 M NaOH containing different concentrations of MAMT at 30°C are shown in Fig. 6. Similar plots were obtained at other temperatures also. As can be seen from Fig. 6, the impedance diagrams show semicircles, indicating that the corrosion process is mainly charge transfer controlled and the additives do not change the reaction mechanism of the corrosion of alloy in sodium hydroxide solution.[45] These results

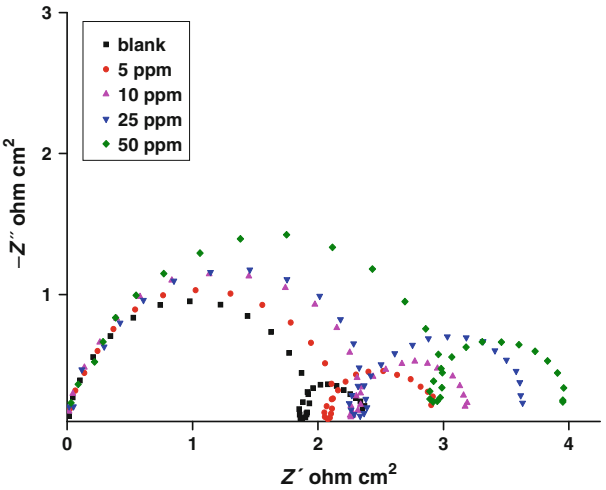

Fig. 6: Nyquist plots for the corrosion of 6061 Al alloy in 0.5 M NaOH at 30°C in the presence of different concentrations of MAMT

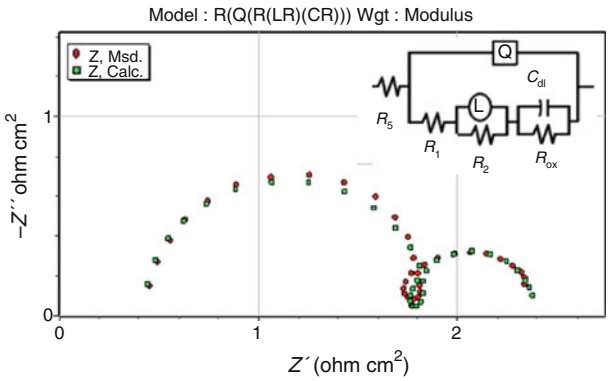

Fig. 7: The electrochemical equivalent circuit used for the simulation of impedance data for the corrosion of 6061 Al alloy in 0.5 M NaOH

support those of polarization measurements, that the inhibitor does not alter the mechanism of electrochemical reactions responsible for the corrosion. It inhibits corrosion primarily through its adsorption on the metal surface.[46]

The impedance spectra manifest into two capacitive semicircles, separated by a small inductive loop at intermediate frequencies. The high-frequency capacitive loop could be assigned to the charge transfer of the corrosion process and to the formation of the oxide layer.[47,48] The oxide film is considered to be a parallel circuit of a resistor due to the ionic conduction in the oxide film and a capacitor due to its dielectric properties. The capacitive loop is corresponding to the interfacial reactions, particularly, the reaction of aluminum oxidation at the metal/oxide/electrolyte interface.[49,50] The process includes the formation of Al^{+} ions at the metal/oxide interface, and their migration through the oxide/solution interface where they are oxidized to Al^{3+}. At the oxide/solution interface, OH^{-} or O^{2-} ions are also formed. The presence of only one loop could be attributed either to the overlapping of the loops of processes, or to the assumption that one process dominates, thereby excluding the other processes.[51] The inductive loop shown in the medium-frequency range might have been caused by the intermediate species generated during Al dissolution process.[52,53] Low-frequency capacitive loop indicated the growth and dissolution of the surface film.

The impedance data were analyzed using an equivalent circuit (EC) that tentatively models the physical processes occurring at the metal-electrolyte interface. The EC consisting of seven elements is depicted in Fig. 7. In this equivalent circuit, R_s is the solution resistance with the value at a high-frequency intercept on the real impedance axis. It has been reported that Al dissolves into the solution in the 3+ oxidation state through the generation of Al^{+} or Al^{2+} intermediate species.[1,54] Therefore, the polarization resistance, R_p, might be represented by the sum of R_1 and R_2 in the equivalent circuit which is parallel to CPE(Q). R_{OX} is the resistance of the native oxide layer; C_{dl} describes the capacitance of the oxide film. This also consists of L in parallel to R_2 but in series with R_1, resulting from the interruption of anodic dissolution of Al by the surface charge buildup.[55]

The semicircles of the impedance spectra for the base alloy are depressed. Deviation of this kind is referred to as frequency dispersion, and has been attributed to inhomogeneities of the solid surfaces.[56] Mansfeld et al.[47,48] have suggested an exponent n in the impedance function as a deviation parameter from the ideal behavior. By this suggestion, the capacitor in the equivalent circuit can be replaced by the so-called constant phase element (CPE), which is a frequency-dependent element and related to surface roughness. The impedance function of a CPE has the following equation[52]:

$$z_{\mathrm{CPE}} = Y_0^{-1}(j\omega)^{-n} \tag{11}$$

where the amplitude Y_0 and n are frequency-independent CPE constant and exponent, respectively, and ω is the angular frequency in rad s^{-1} for which $-Z''$ reaches its maximum value, and $j^2 = -1$, an imaginary number. n is dependent on the surface morphology: $-1 \leq n \leq 1$. Y_0 and n can be calculated by the equations proven by Mansfeld et al.[57]

The double layer capacitances C_{dl}, for a circuit including CPE were calculated from the following equation[58]:

$$C_{\mathrm{dl}} = Y_0(2\pi f_{\max})^{n-1} \tag{12}$$

where f_{max} is the frequency at which the imaginary component of the impedance is maximal. According to

the Helmholtz model,[27] the double-layer capacitance is given by the expression:

$$C_{dl} = \frac{\varepsilon\varepsilon_0}{d} S \tag{13}$$

where d is the thickness of the film, S is the surface area of the electrode, ε_0 is the permittivity of air and ε is the local dielectric constant. The value of C_{dl} decreases due to the adsorption of inhibitor molecules, which displaces water molecules originally adsorbed on the alloy surface and decreases the active surface area. The value of double-layer capacitance decreases with increase in inhibitor concentration indicating that inhibitor molecules function by adsorption at the metal/solution interface, leading to protective film on the alloy surface, and decreasing the extent of the dissolution reaction[59]:

In accordance with the EC given in Fig. 7, the polarization resistance, R_p is given as

$$R_p = R_1 + R_2 \tag{14}$$

The percentage of inhibition efficiency %IE was calculated from the following equation.

$$\%IE = \left[\frac{\left(\frac{1}{R_p}\right)_0 - \left(\frac{1}{R_p}\right)}{\left(\frac{1}{R_p}\right)_0}\right] \times 100 \tag{15}$$

where $(R_p)_0$ and (R_p) are the uninhibited and inhibited polarization resistances, respectively.

AC impedance data of 6061 Al alloy in 0.5 M NaOH in the absence and presence of different concentrations of MAMT are given in Table 5. The value of polarization resistance (R_p) increases and that of the double-layer capacitance (C_{dl}) decreases, with the increase in the concentration of MAMT in the solution, indicating the decrease in the corrosion rate of the base alloy with the increase in MAMT concentration. This is in accordance with the observations from the potentiodynamic measurements.

Table 5: Impedance results for the corrosion of 6061 Al alloy in 0.5 M sodium hydroxide solution in the presence of MAMT at different temperatures

Temperature (°C)	Inhibitor concentration (ppm)	R_p (Ω cm^2)	C_{dl} (F cm^{-2})	IE (%)
30	0	2.86	0.24	–
	5	4.90	0.22	41.6
	10	5.03	0.21	43.0
	25	6.25	0.18	54.2
	50	6.57	0.14	56.4
35	0	2.24	0.25	–
	5	3.68	0.23	39.0
	10	3.83	0.22	41.3
	25	4.85	0.20	53.7
	50	5.14	0.15	56.3
40	0	2.04	0.26	–
	5	3.25	0.25	37.4
	10	3.36	0.23	39.4
	25	3.98	0.21	48.9
	50	4.34	0.16	53.2
45	0	1.75	0.50	–
	5	2.79	0.37	37.1
	10	2.89	0.41	39.4
	25	3.29	0.38	46.7
	50	3.39	0.34	48.4
50	0	1.45	0.53	–
	5	2.21	0.50	34.4
	10	2.29	0.45	36.9
	25	2.65	0.41	45.5
	50	2.79	0.37	48.2

Inhibition mechanism

It is known that, in general, the high inhibition efficiencies are obtained with organic inhibitors in the acid medium, whereas the substances give only nominal inhibition in alkaline solutions. This may be attributed to the high negative potential of aluminum in the alkaline solution which may not be favorable for the adsorption of the organic compounds.[60,61] In the present case of using MAMT as corrosion inhibitor for 6061 Al base alloy in 0.5 M sodium hydroxide, a maximum of about 62% corrosion inhibition of the base alloy is achieved at 30°C. The good inhibition efficiency of MAMT is attributed to the strong adsorption of inhibitor species on the metal surface through the active centers, nitrogen and sulfur atoms. The presence of methyl group in MAMT molecule with + R (resonance) and + I (inductive) effect has a marked effect on the inhibition efficiency of the triazole molecule. This would donate a charge through hyperconjugation and by the inductive effect, thus concentrating the charge density on nitrogen and sulfur atoms—thereby increasing their adsorption at the anodic sites of the metal. In the presence of aggressive hydroxide ions, it is assumed that the inhibitor anions with high charge density compete with anions such as OH^- ions and are preferentially adsorbed at the anodic sites of the metal surface.

The principal cathodic reaction is reduction of water molecules on the aluminum alloy surface according to equations (16) and (17). Adsorption of the inhibitor molecules at the metal surface replaces the water molecules within the electrical double layer to produce a less pronounced dielectric effect,[24] and thus holds up the reaction of surface water molecules and reduces

the rate of hydrogen evolution, thereby affecting the cathodic reactions.

$$H_2O_{(surface)} + e^- \rightleftarrows H + OH^- \quad (16)$$

$$H + H_2O_{(surface)} + e^- \rightleftarrows H_2 + OH^- \quad (17)$$

Scanning electron microscopy

In order to evaluate the effect of corrosion on the surface morphology of the base alloy, SEM analysis was carried out on the samples subjected to corrosion in 0.5 M NaOH solution in the presence and absence of the inhibitors. Figure 8 shows the SEM images of the base alloy. The faceting seen in Fig. 8a is due to the attack of aggressive hydroxide ions, with the specimen undergoing more or less uniform corrosion. Figure 8b depicts the SEM of specimen after 1 h of immersion in 0.5 M NaOH solution in the presence of 50 ppm MAMT at 30°C. It can be seen that MAMT almost completely covers the material surface and protects it from the aggressive media. However, the appearance of incipient damage of the protective layer may be due to the stress produced by growth of the protective film; this permits a free access of aggressive ions to the metal surface.

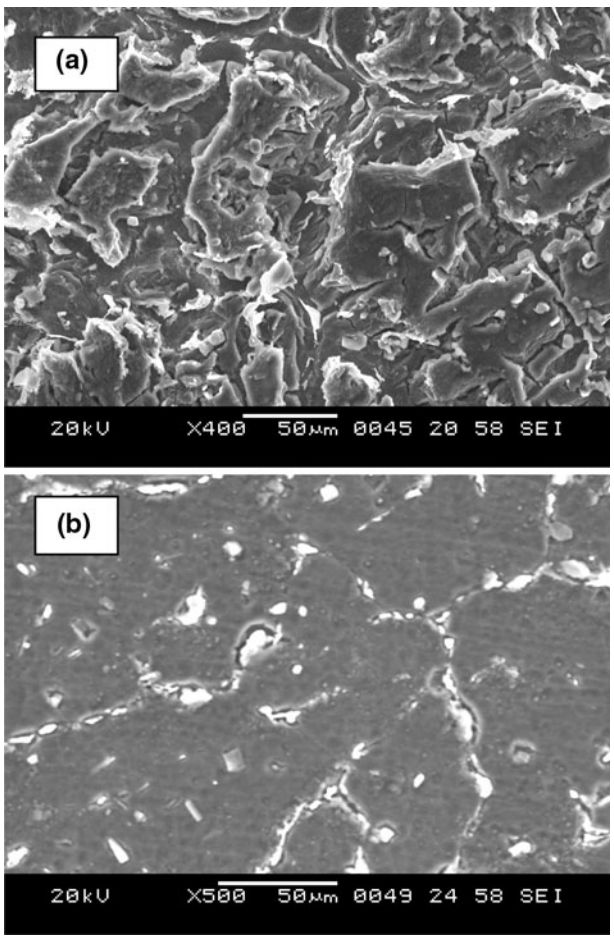

Fig. 8: SEM images of the surfaces of 6061 Al alloy after immersion for 1 h in 0.5 M NaOH solution at 30°C (a) in the absence of MAMT (b) in the presence of 50 ppm MAMT

Conclusions

Potentiodynamic polarization and electrochemical impedance methods were employed to evaluate the ability of MAMT to inhibit corrosion of 6061 Al alloy in 0.5 M NaOH. The principal conclusions are:

- MAMT acts as a good inhibitor for the corrosion of 6061 Al alloy in 0.5 M NaOH solution.
- The inhibition efficiency increases with the increase in inhibitor concentration.
- Inhibition efficiency decreases with the increase in temperature of the medium.
- MAMT behaves as mixed type inhibitor predominantly affecting the cathodic reactions.
- The adsorption of MAMT on the base alloy surface is through physisorption and obeys Langmuir's adsorption isotherm model.
- The adsorption process is exothermic and accompanied by a decrease in enthalpy.
- The inhibition efficiency obtained from potentiodynamic polarization method and EIS technique are in reasonably good agreement.

References

1. Doche, ML, Rameau, JJ, Durand, R, Novel-Cattin, F, ''Electrochemical Behaviour of Aluminium in Concentrated NaOH Solutions.'' *Corros. Sci.*, **41** 805–826 (1999)
2. Moon, S-M, Pyun, S-I, ''The Formation and Dissolution of Anodic Oxide Films on Pure Aluminium in Alkaline Solution.'' *Electrochim. Acta*, **44** 2445–2454 (1999)
3. Henryk, S, Martin, MDJ, ''The Applications of 1-Hydroxyimidazole-3-N-Oxides as Aluminium Corrosion Inhibitors in Alkaline Solutions.'' *Corros. Sci.*, **33** 1967–1978 (1992)
4. Fouda, AS, AI-Sarawy, AA, Sh. Ahmed, F, EI-Abbasy, HM, ''Corrosion Inhibition of Aluminium 6063 Using Some Pharmaceutical Compounds.'' *Corros. Sci.*, **51** 485–492 (2009)
5. Nitin, WP, Jyothirmayi, A, RamaKrishna, L, Sundararajan, G, ''Effect of Micro Arc Oxidation Coatings on Corrosion Resistance of 6061-Al Alloy.'' *JMEPEG*, **17** 708–713 (2008)
6. Davis, J, *Corrosion Understanding the Basics*. ASM International, Materials Park, OH, 2000
7. AI-Kharafi, FM, Badawy, WA, ''Inhibition of Corrosion of Al 6061, Aluminium, and an Aluminium–Copper Alloy in Chloride-Free Aqueous Media. Part-2. Behavior in Basic solutions.'' *Corrosion*, **5** 377–385 (1997)
8. Talati, JD, Modi, RM, ''p-Substituted Phenols as Corrosion Inhibitors for Aluminium–Copper Alloy in Sodium Hydroxide.'' *Corros. Sci.*, **19** 35–48 (1979)

9. Bereket, G, Pinarbasi, A, ''Electrochemical Thermodynamic and Kinetic Studies of the Behavior of Aluminium in Hydrochloric Acid Containing Various Benzotriazole Derivatives.'' *Corros. Eng. Sci. Technol.*, **39** 308–312 (2004)
10. Oguzie, EE, Okolue, BN, Ogukwe, CE, Unaegbu, C, ''Corrosion Inhibition and Adsorption Behaviour of Bismark Brown Dye on Aluminium in Sodium Hydroxide Solution.'' *Mater. Lett.*, **60** 3376–3378 (2006)
11. Satpati, AK, Ravindran, PV, ''Electrochemical Study of the Inhibition of Corrosion of Stainless Steel by 1,2,3-Benzotriazole in Acidic Media.'' *Mater. Chem. Phys.*, **109** 352–359 (2008)
12. Branzoi, V, Golgovici, F, Branzoi, F, ''Aluminium Corrosion in Hydrochloric Acid Solutions and the Effect of Some Organic Inhibitors.'' *Mater. Chem. Phys.*, **78** 122–131 (2002)
13. Moussa, MN, Fouda, AS, Taha, FI, Elnenaa, A, ''Some Thiosemicarbazide Derivatives as Corrosion Inhibitors for Aluminium in Sodium Hydroxide Solution.'' *Bull. Korean Chem. Soc.*, **9** 191–195 (1988)
14. Grubac, Z, Babic, R, Metikos-Hukovic, M, ''Application of Substituted N-Arylpyrroles in the Corrosion Protection of Aluminium in Hydrochloric Acid.'' *J. Appl. Electrochem.*, **32** 431–438 (2002)
15. Sayed Abd EI Rehim, S, Hamdi Hassan, H, Mohammed Amin, A, ''The Corrosion Inhibition Study of Sodium Dodecyl Benzene Sulphonate to Aluminium and Its Alloys in 1.0 M HCl Solution.'' *Mater. Chem. Phys.*, **78** 337–348 (2003)
16. Abdallah, M, ''Antibacterial Drugs as Corrosion Inhibitors for Corrosion of Aluminium in Hydrochloric Solution.'' *Corros. Sci.*, **46** 1981–1996 (2004)
17. Suma, AR, Padmalatha, Nayak, J, Shetty, AN, ''3-Methyl-4-amino-5-mercapto-1,2,4-triazole as Inhibitor of Corrosion of 6061 Al-15 Vol.Pct. SiCp Composite.'' *J. Metall. Mater. Sci.*, **47** 51–57 (2005)
18. Bektas, H, Karaali, N, Sahin, D, Demirbas, A, Karaoglu, SA, ''Synthesis and Antimicrobial Activities of Some New 1,2,4-Triazole Derivatives.'' *Molecules*, **15** 2427–2438 (2010)
19. Poornima, T, Nayak, J, Shetty, AN, ''3,4-Dimethoxybenzaldehydethiosemicarbazone as Corrosion Inhibitor for Aged 18 Ni 250 Grade Maraging Steel in 0.5 M Sulfuric Acid.'' *J. Appl. Electrochem.*, **41** 223–233 (2011)
20. Gadiyar, HRA, ''Studies on Heterocyclic Thiols as Complexing Agents, Analytical Reagents and Corrosion Inhibitors.'' Thesis, Mangalore University, 1986
21. Fontana, MG, *Corrosion Engineering*, 3rd ed. McGraw-Hill, Singapore, 1987
22. Ferreira, ES, Gianocomelli, C, Giacomelli, FC, Spinelli, A, ''Evaluation of the Inhibitor Effect of L-Ascorbic Acid on the Corrosion of Mild Steel.'' *Mater. Chem. Phys.*, **83** 129–134 (2004)
23. Li, WH, He, Q, Pei, CL, Hou, BR, ''Some New Triazole Derivatives as Inhibitors for Mild Steel Corrosion in Acidic Medium.'' *J. Appl. Electrochem.*, **38** 289–295 (2008)
24. Yazdad, AR, Shahrabi, T, Hosseini, MG, ''Inhibition of 3003 Aluminium Alloy Corrosion by Propargyl Alcohol and Tartrate Ion and Their Synergistic Effects in 0.5% NaCl Solution.'' *Mater. Chem. Phys.*, **109** 199–205 (2008)
25. Rosliza, R, Wan Nik, WB, ''Improvement of Corrosion Resistance of AA6061 Alloy by Tapioca Starch in Seawater.'' *Curr. Appl. Phys.*, **10** 221–229 (2010)
26. Li, W, He, Q, Pei, C, Hou, B, ''Experimental and Theoretical Investigation of the Adsorption Behaviour of New Triazole Derivatives as Inhibitors for Mild Steel Corrosion in Acid Media.'' *Electrochim. Acta*, **52** 6386–6394 (2007)
27. McCafferty, E, Hackerman, N, ''Concentrated Acidic Chloride Solutions.'' *J. Electrochem. Soc.*, **119** 999–1009 (1972)
28. Bentiss, F, Lebrini, M, Lagrenée, M, ''Thermodynamic Characterization of Metal Dissolution and Inhibitor Adsorption Processes in Mild Steel/2,5-bis(n-thienyl)-1,3,4-thiadiazoles/Hydrochloric Acid System.'' *Corros. Sci.*, **47** 2915–2931 (2005)
29. Schorr, M, Yahalom, J, ''The Significance of the Energy of Activation for the Dissolution Reaction of Metal in Acids.'' *Corros. Sci.*, **12** 867–868 (1972)
30. Antropov, LI, ''A Correlation Between Kinetics of Corrosion and the Mechanism of Inhibition by Organic Compounds.'' *Corros. Sci.*, **7** 607–620 (1967)
31. Ashassi-Sorkhabi, H, Shaabani, B, Seifzadeh, D, ''Corrosion Inhibition of Mild Steel by Some Schiff Base Compounds in HCl.'' *Appl. Surf. Sci.*, **239** 154–164 (2005)
32. Osman, MM, El-Ghazawy, RA, Al-Sabagh, AM, ''Corrosion Inhibitor of Some Surfactants Derived from Maleic–Oleic Acid Adduct on Mild Steel in 1 M H_2SO_4.'' *Mater. Chem. Phys.*, **80** 55–62 (2003)
33. Mansfeld, F, *Corrosion Mechanism*. Marcel Dekkar, New York, 1987
34. Sahin, M, Bilgic, S, Yilmaz, H, ''The Inhibition Effects of Some Cyclic Nitrogen Compounds on the Corrosion of the Steel in NaCl Mediums.'' *Appl. Surf. Sci.*, **195** 1–7 (2002)
35. Ateya, B, El-Anadouli, BE, El-Nizamy, FM, ''The Adsorption of Thioureaon Mild Steel.'' *Corros. Sci.*, **24** 509–515 (1984)
36. Oguzie, EE, Njoku, VO, Enenebeak, CK, Akalezi, CO, Obi, C, ''Effect of Hexamethylpararosaniline Chloride (Crystal Violet) on Mild Steel Corrosion in Acidic Media.'' *Corros. Sci.*, **50** 3480–3486 (2008)
37. Sethi, T, Chaturvedi, A, Upadhyay, RK, Mathur, SP, ''Corrosion Inhibitory Effects of Some Schiff's Bases on Mild Steel in Acid Media.'' *J. Chil. Chem. Soc.*, **52** 1206–1213 (2007)
38. Olivares, O, Likhanova, NV, Gomez, B, Navarrete, J, Llanos-Serrano, ME, Arce, E, Hallen, JM, ''Electrochemical and XPS Studies of Decylamides of α-Aminoacids Adsorption on Carbon Steel in Acidic Environment.'' *Appl. Surf. Sci.*, **252** 2894–2909 (2006)
39. Kliskic, M, Radosevic, J, Gudic, S, Katalinic, V, ''Aqueous Extract of *Rosmarinus officinalis* L. as Inhibitor of Al–Mg Alloy Corrosion in Chloride Solution.'' *J. Appl. Electrochem.*, **30** 823–830 (2000)
40. EI-Sayed, A-R, Shaker, MA, Abd EI-Lateef, HM, ''Corrosion Inhibition of Tin, Indium and Tin–Indium Alloys by Adenine or Adenosine in Hydrochloric Acid Solution.'' *Corros. Sci.*, **52** 72–81 (2010)
41. Umoren, SA, Ebenso, EE, Okafor, PC, Ekpe, UJ, Ogbobe, O, ''Synergetic Effect of Halide Ions and Polyethylene Glycol on the Corrosion Inhibition of Aluminium in Alkaline Medium.'' *J. Appl. Polym. Sci.*, **103** 2810–2816 (2007)
42. Singh, AK, Quraishi, MA, ''The Effect of Some Bis-Thiadiazole Derivatives on the Corrosion of Mild Steel in Hydrochloric Acid.'' *Corros. Sci.*, **52** 152–160 (2010)
43. Durnie, W, Marco, RD, Jefferson, A, Kinsella, B, ''Development of a Structure Activity Relationship for Oil Field Corrosion Inhibitors.'' *J. Electrochem. Soc.*, **146** 1751–1756 (1999)
44. Martinez, S, Stern, I, ''Thermodynamic Characterization of Metal Dissolution and Inhibitor Adsorption Processes in the Low Carbon Steel/Mimosa Tannin/Sulfuric Acid System.'' *Appl. Surf. Sci.*, **199** 83–89 (2002)
45. Libin, T, Guannan, M, Guangheng, L, ''The Effect of Neutral Red on the Corrosion Inhibition of Cold Rolled

Steel in 1.0 M Hydrochloric Acid.'' *Corros. Sci.*, **45** 2251–2262 (2003)
46. Amin, MA, Abd El-Rehim, SS, El-Sherbini, EEF, Bayyomi, RS, ''The Inhibition of Low Carbon Steel Corrosion in Hydrochloric Acid Solutions by Succinic Acid. Part 1. Weight Loss. Polarization, EIS, PZC, EDX and SEM Studies.'' *Electrochim. Acta*, **52** 3588–3600 (2007)
47. Mansfeld, F, Lin, S, Kim, S, Shih, H, ''Pitting and Surface Modification of SiC/Al.'' *Corros. Sci.*, **27** 997–1000 (1987)
48. Mansfeld, F, Lin, S, Kim, S, Shih, H, ''Electrochemical Impedance Spectroscopy as a Monitoring Tool for Passivation and Localized Corrosion of Aluminium Alloys.'' *Mater. Corros.*, **39** 487–492 (1988)
49. Brett, CMA, ''The Application of Electrochemical Impedance Techniques to Aluminium Corrosion in Acidic Chloride Solution.'' *J. Appl. Electrochem.*, **20** 1000–1003 (1990)
50. Brett, CMA, ''On the Electrochemical Behaviour of Aluminium in Acidic Chloride Solution.'' *Corros. Sci.*, **33** 203–210 (1992)
51. Wit, JH, Lenderink, HJW, ''Electrochemical Impedance Spectroscopy as a Tool to Obtain Mechanistic Information on the Passive Behaviour of Aluminium.'' *Electrochim. Acta*, **41** 1111–1119 (1996)
52. Lenderink, HJW, Linden, MVD, De Wit, JHW, ''Corrosion of Aluminium in Acidic and Neutral Solutions.'' *Electrochim. Acta*, **38** 1989–1992 (1993)
53. Macdonald, DD, Real, S, Smeldley, SI, Urquidi-Macdonald, M, ''Evaluation of Alloy Anodes for Aluminium-Air Battery.'' *J. Electrochem. Soc.*, **135** 2410–2414 (1988)
54. Desai, MN, Desai, SM, ''Inhibition of the Corrosion of Al-3s in NaOH.'' *Corros. Sci.*, **10** 233–237 (1979)
55. Lee, KK, Kim, KB, ''Electrochemical Impedance Characteristics of Pure Al and Al-Sn Alloys in NaOH Solution.'' *Corros. Sci.*, **43** 561–575 (2001)
56. Jutner, K, ''Electrochemical Impedance Spectroscopy (EIS) of Corrosion Processes on Inhomogeneous Surfaces.'' *Electrochim. Acta*, **35** 1501–1508 (1990)
57. Mansfeld, F, Tsai, CH, Shih, H, In: Munn, RS (ed.) *Computer Modeling in Corrosion*. ASTM, Philadelphia, 1992
58. Hsu, CH, Mansfeld, F, ''Concerning the Conversion of Constant Phase Element Parameter into a Capacitance.'' *Corrosion*, **57** 747–748 (2001)
59. Bentiss, F, Traisnel, M, Lagrenee, M, ''The Substituted 1,3,4-Oxadiazole: A New Class of Corrosion Inhibitors of Mild Steel in Acidic Media.'' *Corros. Sci.*, **42** 127–146 (2000)
60. Fouda, AS, Elbaz, AM, Mousa, MN, ''Mechanism of the Inhibition Afforded by Some Hydrazone Oxime Derivatives Towards Aluminium in 2 M NaOH Solution.'' *Qatar. Univ. Sci. J.*, **11** 95–111 (1991)
61. Onuchukwu, AI, ''Corrosion Inhibition of Aluminium in Alkaline Medium. I. Influence of Hard Bases.'' *Mater. Chem. Phys.*, **20** 323–332 (1988)